Biodegradable Poly(L-lactic acid)/TiO_2 Nanocomposites: Thermal Properties and Degradation

Aleksandra Buzarovska, Anita Grozdanov

Faculty of Technology and Metallurgy, St Cyril and Methodius University, Rudjer Boskovic 16, 1000 Skopje, Macedonia

Received 2 June 2010; accepted 20 April 2011
DOI 10.1002/app.34729
Published online 23 August 2011 in Wiley Online Library (wileyonlinelibrary.com).

ABSTRACT: Poly(L-lactic acid)-titanium dioxide nanocomposites (with various loadings of TiO_2: 0.5, 1, 2, 5, and 10 wt %) were produced by solution casting method. The influence of TiO_2 on thermal properties and crystallinity of PLA was investigated by DSC and FTIR spectroscopy. The TiO_2 nano filler has no significant influence on the characteristic temperatures (T_g, T_c, and T_m), but has high impact on the crystallinity of these systems. The degree of crystallinity X_c significantly increases for PLA nanocomposites loaded with up to 5 wt % of TiO_2, while for 10 wt % load of TiO_2 it drops below X_c of the pure resin. The degradation of the prepared composites was evaluated hydrolytically in 1*N* NaOH, enzymatically in α-amylase solutions, and under UV irradiation. The catalytic effect of TiO_2 nano particles on the degradation processes under UV light exposure ($\lambda = 365$ nm) and hydrolytic degradation was confirmed with the increase of the filler content. The opposite effect was identified in enzymatic degradation experiments. © 2011 Wiley Periodicals, Inc. J Appl Polym Sci 123: 2187–2193, 2012

Key words: poly (L-lactic acid); TiO_2; degradation

INTRODUCTION

Environmentally friendly polymers (such as polylactic acid) have attracted significant interest in the recent years.[1,2] PLA is fully biodegradable polymer resin when composted in a large-scale operation with temperatures above 60°C. Its glass transition temperature (T_g) around 60°C is one of the reasons that PLA does not biodegrade readily at temperatures less than its T_g.[3] A common disadvantage of this polymer is its slow degradation rate due to higher crystallinity and poor hydrophilicity.

PLA is widely used as a drug delivery system due to its excellent biocompatibility and biodegradability.[4,5]

A wider use of PLA in various applications requires further material development to achieve the necessary properties such as heat stability, improved mechanical, and barrier properties as well as controlled degradation. The unfavorable hydrolytic degradation rate often limits the PLA application. Considerable efforts have been made to control (usually accelerate) the hydrolytic degradation rate.[6,7] Degradation rates could be controlled by addition of plasticizers and additives (especially those in nanosize[8]). Although biodegradation of PLA is advanced in the ground, where moisture and microorganisms exist, still a period longer than 2 months is needed for decomposition,[9] while biodegradation does not advance in air. As a solution, by adding photodegradability to a biodegradable polymer, degradability can be efficiently promoted under any conditions.[10–13]

The incorporation of nanoparticles is an effective tool to modify the polymer resin properties and to control the degradation process in various media.[14]

The TiO_2 nanoparticles are interesting nanomaterial due to its photocatalytic and bacteriostatic activity.[15] For practical photocatalytic application, it is more advantageous to immobilize TiO_2 in certain polymer matrix. It has been reported that by using TiO_2 nanoparticles in nanocomposites with organic polymers, a substantial increase in degradability under solar or UV irradiation could be achieved.[16,17] Zhuang et al. have used *in situ* polymerization method to prepare TiO_2/polylactide (PLA) nanocomposites with different content of TiO_2.[18] Improved thermal and mechanical properties were identified at 3 wt % of TiO_2. It has been reported that TiO_2-filled composites show higher degradability when exposed to UV light radiation and solution degradation experiments. Song et al. have adopted PLA/TiO_2 nanofibers as a new nanomaterial with good biocompatibility and large surface area of the composites.[19] Nakayama et al. reported improved photocatalytic activity of modified TiO_2 nano particles, independent of the filler content.[20]

Correspondence to: A. Buzarovska (abuzar@tmf.ukim.edu.mk).

In this work we have studied nanocomposites made by incorporation of TiO_2 nanoparticles of different concentrations in poly(L-lactic acid). We have examined the influence of TiO_2 nano filler on thermal properties, crystallinity and degradation of PLA resin in various media.

EXPERIMENTAL

Materials

Poly(L-lactic acid) with molecular weight M_w = 100,000, product of Biomer (Krailling, Germany) and TiO_2, Anatase P25 (Degussa AG, Germany) with particle size of 21 nm were used in this research. Chloroform (Merck) was employed as solvent. α-amylase from *Bacillus subtilis* was purchased from Fluka-Biochemica (ς-Aldrich, Switzerland). NaOH was product of Alkaloid (Alkaloid, Skopje, Macedonia).

Composite preparation

PLA/TiO_2 composites with appropriate percentage of TiO_2 (0.5, 1, 2, 5, and 10 wt %) were prepared by solvent-casting method. The polymer was dissolved in hot chloroform (10% w/v) by stirring. TiO_2 particles were added to the polymer solutions and rigorously stirred for 1 h. The PLA/TiO_2 dispersions were additionally ultrasonically treated for 2 h using ultrasonic bath with frequency of 42 kHz. The treated dispersions were poured onto Petri dishes, and the solvent was allowed to evaporate under constant influence of ultrasound. The films were dried to constant mass in a vacuum oven for ~ 24 h. Pure PLA and nanocomposite films had uniform thickness of 200 μm.

Scanning electron microscopy (SEM)

Scanning electron microscopy (SEM) micrographs of TiO_2/PLA nanocomposites were obtained using STEM module—microscope, FEI-Quanta 200 FEG type (EDS-Oxford Inca Energy System 250) equipped with INCAx-act LN2-free detector at 1 keV operating voltage. Nanocomposite samples have been prepared by using sputtering apparatus for metallizing the surfaces with Au-Pd alloy.

Differential scanning calorimetry (DSC)

Nonisothermal crystallization of TiO_2 filled composites was followed using PERKIN ELMER DSC-7 (Wellesley, MA). The weights of all samples were ~ 7 mg. The samples were heated to 200°C at a heating rate of 10° min^{-1} and held for 3 min to erase the previous thermal history (I run). The samples were nonisothermally crystallized by cooling from 200°C to −30°C at a cooling rate of 5° min^{-1}. The crystallized samples were reheated again in the same temperature region (II run) with a heating rate of 10° min^{-1} (II run). The same thermal methodology was applied for UV irradiated films as well.

Fourier-transform infrared spectroscopy (FTIR)

The FTIR spectra of PLA-TiO_2 composite films were measured by attenuated total reflection (ATR) method (64 scans were averaged at a resolution of 4 cm^{-1}) with Perkin–Elmer Spectrum 100 FTIR instrument.

FTIR spectroscopy was used to determine the influence of the filler on the crystalline sensitive bands and to observe their behavior after certain time of UV degradation.

Degradation experiments

UV degradation

The PLA films with average thickness of 200 μm, and various concentrations of TiO_2 were exposed to UV monochromatic light at λ = 365 nm during various times of exposure. The distance between the UV lamp and the samples was 2 cm, and the intensity of the measured light was 1950 μW cm^{-2}. The weight loss (W_{loss}) was calculated using the expression:

$$W_{loss}(\%) = \frac{W_0 - W_t}{W_0} \times 100$$

where W_0 is the initial weight of polymer film and W_t is the weight at time t of exposure under UV light.

Hydrolytic degradation

Hydrolytic degradation of the films (10 × 10 mm^2) was carried out at 37°C in small bottles containing 1 mol dm^{-3} NaOH solutions. Following the incubation for a given time, the films were periodically removed, washed with distilled water, dried in vacuum for 2 days, and therefore used to determine the mass loss.

Enzymatic degradation

The enzymatic degradation was followed in α-amylase solutions (5 U mg^{-1} polymer) at 37°C. The amylase solution was replaced every 24 h to confirm its equal activity during the degradation process. The weight losses versus time plots were obtained in the same manner as for the UV degradation experiments. Before measuring the weight loss, composite films were washed with distilled water and dried in vacuum oven to a constant weight.

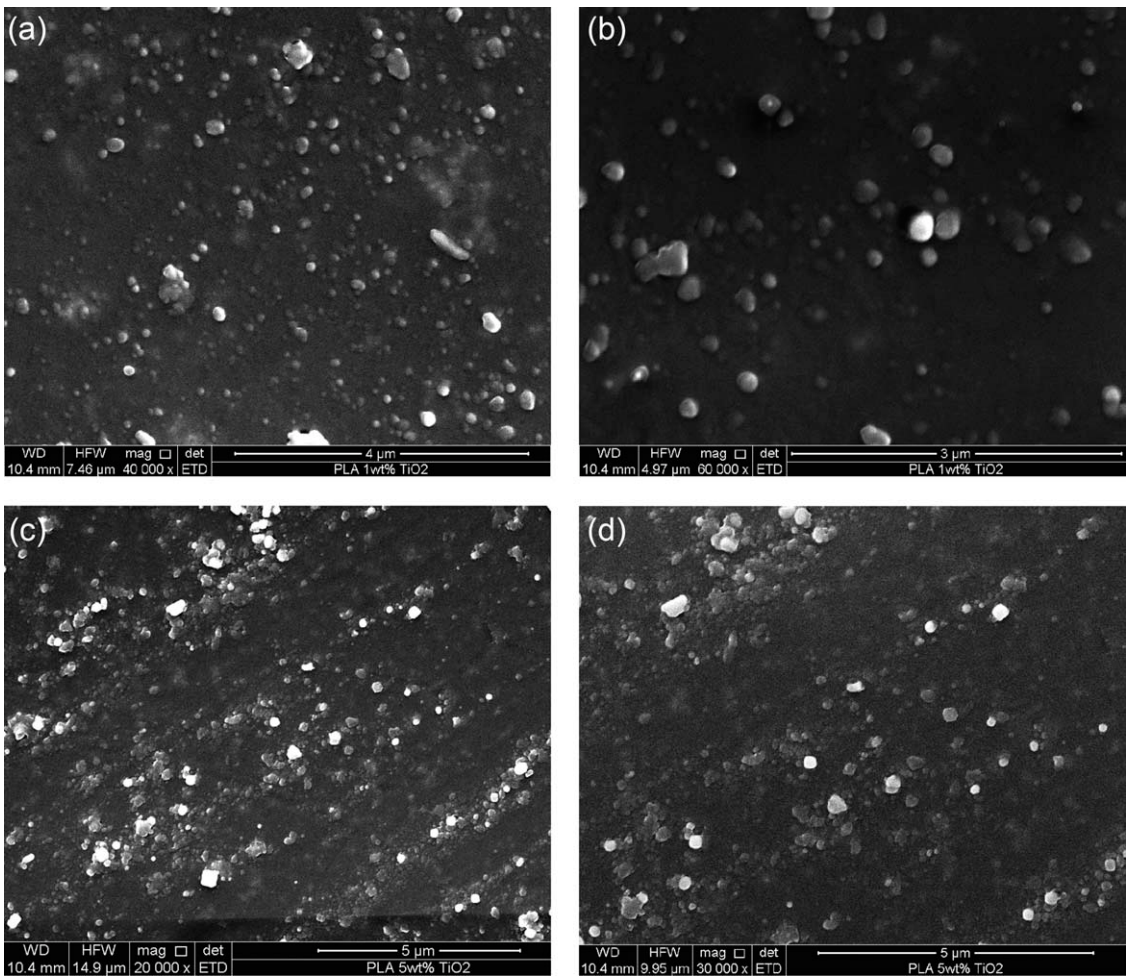

Figure 1 (a) SEM image of PLA-1, magnification ×40,000. (b) SEM image of PLA-1, magnification ×60,000. (c) SEM image of PLA-5, magnification ×20,000. (d) SEM image of PLA-5, magnification ×30,000.

RESULTS AND DISCUSSION

Morphology

The SEM analysis of the TiO_2/PLA nanocomposite was performed to investigate the dispersion and distribution of TiO_2 nanoparticles within the biodegradable matrix. The SEM photographs of the PLA loaded with 1 and 5 wt % TiO_2 are shown in Figure 1. Besides the fact that TiO_2 nanoparticles were used as received, SEM images show that TiO_2 nanoparticles are almost completely embedded in the PLA matrix. It can be observed that the oxide nanoparticles are well dispersed in the material but with a tendency for aggregation. The size of the aggregates is smaller than 0.2 µm. The tendency to aggregation can be explained by the fact that no surface treatment was performed on the oxide particles, and nanocomposite preparation by solution-mixing and direct dispersing of TiO_2 nanoparticles in PLA solution was used. Regarding the nanoparticle distribution, TiO_2 nanoparticles have shown line orientation that can be favorable for certain applications. The dispersion states of TiO_2 in the polymer matrix directly affect physical properties of the nanocomposites, which will be enhanced by effective use of their extraordinary properties obtained at the individual nanoparticle level.

Thermal properties

Nanoparticles could have considerable influence on the crystallization process, acting as nucleating agents.[21]

The crystallization exotherms for pure polymer resin and its composite films with TiO_2 are shown in Figure 2. At a constant cooling rate of 5° min^{-1}, crystallization peak temperatures (T_c) for all investigated samples are around 100°C, showing considerable independence of the TiO_2 content. As listed in Table I, the degree of crystallinity (X_c) of the PLA/TiO_2 films was increased with the increase of TiO_2 content (up to 5 wt % of TiO_2), while X_c for PLA-10 drops below X_c of the pure resin. The degree of crystallinity was calculated according to the relation

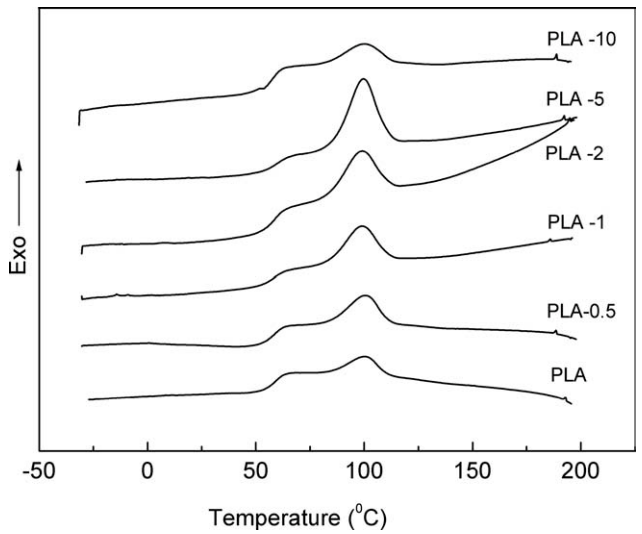

Figure 2 Crystallization exotherms for PLA/TiO_2 composite films.

$X_c = \Delta H_f / \Delta H_f^o$, where ΔH_f is the experimental enthalpy of fusion, and ΔH_f^o (taken as 93.2 J g^{-122}) is the enthalpy of melting of an ideal crystal. As shown in Table I, the overall crystallization time t_c slightly increased only in PLA-10 composite film, while for the other samples t_c is almost constant. The overall crystallization time (t_c) was calculated as $t_c = (T_s - T_e)/v$, where v is the cooling rate of 5° min^{-1}, and T_s and T_e are the initial and end crystallization temperatures respectively. Generally, the increased values of X_c and shifting of T_c to higher values, as well as less supercooling (lower crystallization times), are the key aspects to consider certain filler as nucleating agent.[23] In these systems, PLA crystallizes with nearly constant supercooling, and increased degree of crystallinity (up to 5 wt % of TiO_2). This might be an indication that nanoparticles do not play active role in the heterogeneous nucleation of polymer resin. Homogenous nucleation probably took place, started spontaneously by chain aggregation that actually needs longer times. The increased X_cs are not in a correlation with the corresponding supercoolings, but could be an indication that the nanoparticles could also have significant influence on the crystallization process. Additionally this phenomenon could be ascribed to the TiO_2 nanoparticles that disrupt the regularity of the PLA chain structure. Further experiments are in progress to clarify the nucleation mechanism of PLA/TiO_2 systems and the influence of TiO_2 content on the secondary crystallization process.

TABLE I
DSC Data for PLA and its Composite with TiO_2

Sample	T_c (°C)	t_c (min)	X_c (%)	T_g (°C)	T_{cc} (°C)	T_m (°C)
PLA	100	5.4	7.4	61	117	170
PLA-0.5	100	5.6	10.0	61	113	171
PLA-1	99	5.6	14.5	61	110	171
PLA-2	99	5.5	20.9	61	112	171
PLA-5	99	5.1	10.9	61	104	171
PLA-10	101	6.2	6.5	61	121	169

The melting endotherms of the crystallized samples are shown in Figure 3. According to these measurements, the glass transition (T_g) and melting (T_m) temperatures are around 61 and 170°C, respectively, indicating that nano filler has no effect on the mobility of macromolecular chains in all investigated samples. On the other hand, the process of cold crystallization is significantly affected by the increasing content of TiO_2. With the increase of TiO_2 content (up to 5 wt %) the cold crystallization peak (T_{cc}) is shifted to lower temperature, while for PLA-5 and PLA-10, the T_{cc} peaks are close to those characteristic for PLA. In spite of the fact that the cold crystallization process has received limited scientific attention (mostly from practical point of view), this phase transition process could be an important indication of the crystal reorganizations during the heating process.

FTIR spectroscopy characterization of crystallinity

FTIR spectroscopy was used to detect the influence of nano filler content on the crystalline sensitive bands and to determine the crystallinity indices. Figure 4 shows FTIR spectra of PLA and its composites filled with TiO_2 nanoparticles. A strong absorbance band at 1748 cm^{-1}, attributed to the stretching vibrations of amorphous carbonyl groups is shown in spectra of all samples.[24] Only in PLA-10 sample a shoulder at 1755 cm^{-1} (a crystalline sensitive band due to C=O stretching vibrations) could be

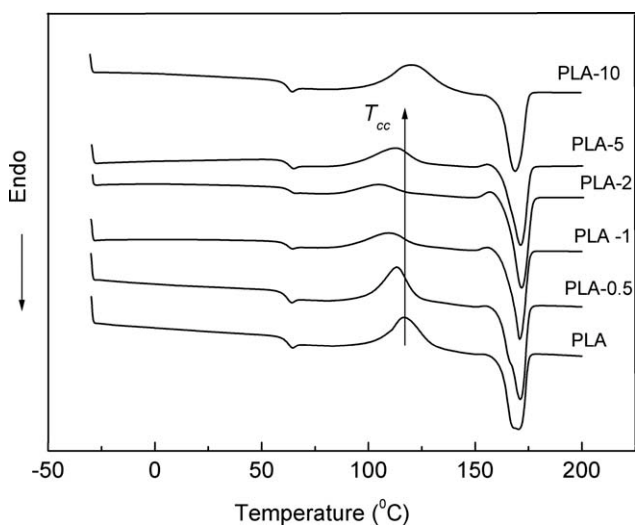

Figure 3 Second heating runs for PLA and its composites with TiO_2.

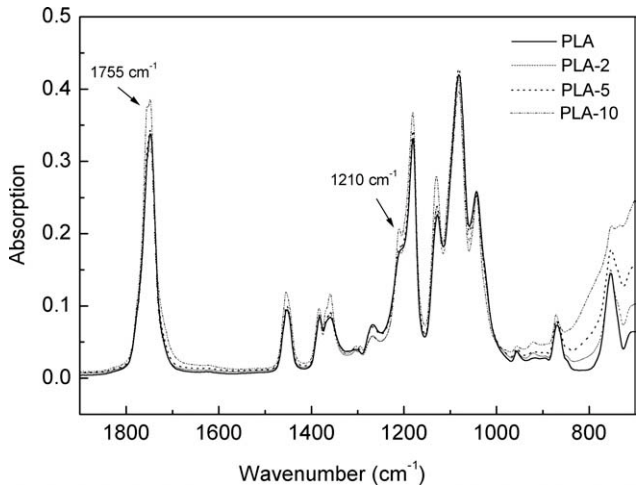

Figure 4 FTIR-ATR spectra of PLA and its composite films with TiO_2.

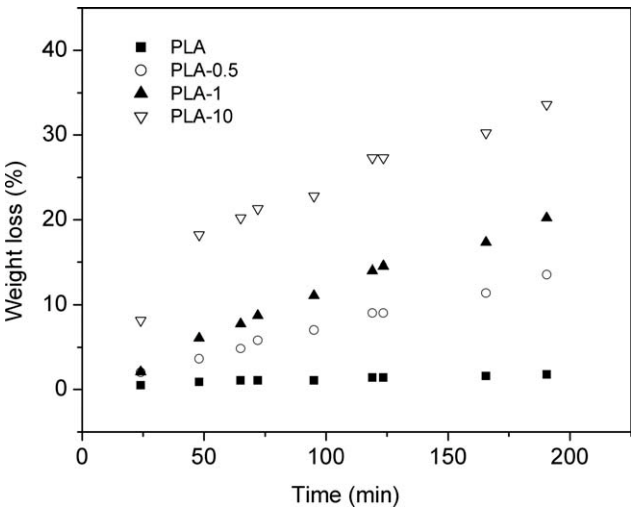

Figure 5 Weight loss/irradiation time dependence for PLA composite films.

identified. The other observed bands, positioned at 1452 and 1382 cm^{-1}, are due to the CH_3 asymmetric and symmetric deformations. The strong absorption band located at 1180 cm^{-1} is due to C—O—C stretching mode, while a shoulder positioned at 1210 cm^{-1} is attributed to C—O—C stretching characteristic for the crystalline phase. In case of PLA composites it is obvious that TiO_2 has influence on the characteristic band intensities. The crystallinity index (CI) was determined by normalizing the 1180 cm^{-1} band to that of the 1382 cm^{-1}, which was found from the literature to be sensitive to the degree of crystallinity.[25] The CI is a relative measure of crystallinity and can be used to compare crystallinity between different samples. The estimated CI's given in Table II are actually average values of five different FTIR measurements within the certain film. CI has slightly increased only for PLA-10, while for other samples CI is around 0.16.

Photodegradation properties of PLA composite films

PLA composites filled with TiO_2 particles were exposed to UV light (λ = 365 nm). The typical graphs weight losses versus time of UV exposure are shown in Figure 5. Linear variation could be identified in all filled composites and in pure resin as well. The degradation rates could be obtained by linear fitting of the presented data as a slope of the plots presented in Figure 5. The degradation rates of 0.0068, 0.062, 0.10, 0.13%/h for PLA, PLA-0.5, PLA-1, and PLA-10 respectively, clearly show that the degradation is significantly faster in PLA composites with higher content of TiO_2 due to the photocatalytic activity of the filler. Contrary to this, Nakayama et al. have reported that the degrees of weight loss in PLA matrices owing to UV irradiation did not depend on the amount of added functionalized TiO_2 nanoparticles.[20]

The DSC data obtained from the thermograms for UV irradiated samples (after 190 h of irradiation) are collected in Table III. No considerable changes in crystallization peaks (Fig. 6) are visible since their positions are around 99°C and are close to T_c of nondegraded samples. Pronounced changes in crystallinity indices of UV degraded samples are detectable when compared to those obtained for nondegraded ones. The X_c increased almost double in all TiO_2 filled composites, while the X_cs of irradiated PLA resin is slightly higher than X_c of nonirradiated PLA. Also very slight decrease of the T_gs could be identified in UV treated filled samples, indicating slightly increased mobility of PLA chains (Table III).

TABLE II
CIs Derived from the I_{1180}/I_{1382} Intensity Ratio with FTIR Absorption Data

Sample	CI	CI after (190 h of UV irradiation)
PLA	0.16	0.16
PLA-0.5	0.17	0.16
PLA-1	0.17	0.16
PLA-2	0.16	0.16
PLA-5	0.16	0.15
PLA-10	0.18	0.17

TABLE III
DSC Data of UV Irradiated PLA Composite Films

Sample	T_c (°C)	t_c (min)	X_c (%)	T_g (°C)	T_{cc} (°C)	T_m (°C)
PLA	101	6.2	8.7	61	116	170
PLA-0.5	99	5.1	28.8	59	100	168
PLA-1	98	5.0	30.3	56	100	166
PLA-10	100	6.4	18.5	59	110	169

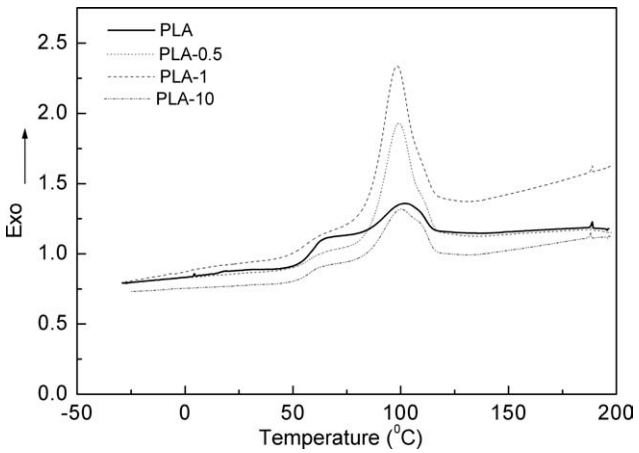

Figure 6 Crystallization exotherms of UV irradiated PLA/TiO_2 composite films.

The mobility of polylactic chains is probably increased due to the lowering of the molecular weight as a result of degradation. The increased crystallinity might be also caused by degradation of PLA polymer chains, since low molecular weight polymers have high crystallinity and high crystallization rate.[26]

There is also another hypothesis that the degradation preferably occurs in the amorphous parts of PLA, thus increasing the overall crystallinity indices.[27] From the FTIR spectra of UV treated films it is observed that the intensities of all absorption bands are decreased when compared to those, characteristic for nontreated samples [Fig. 7(a,b)].

The estimated crystalinity indices from the FTIR measurements, obtained as intensity ratio between the bands located on 1453 and 1180 cm^{-1}, show almost identical values as nontreated ones (Table II). From all the above-presented data, TiO_2 nano particles affect the process of degradation photocatalytically.

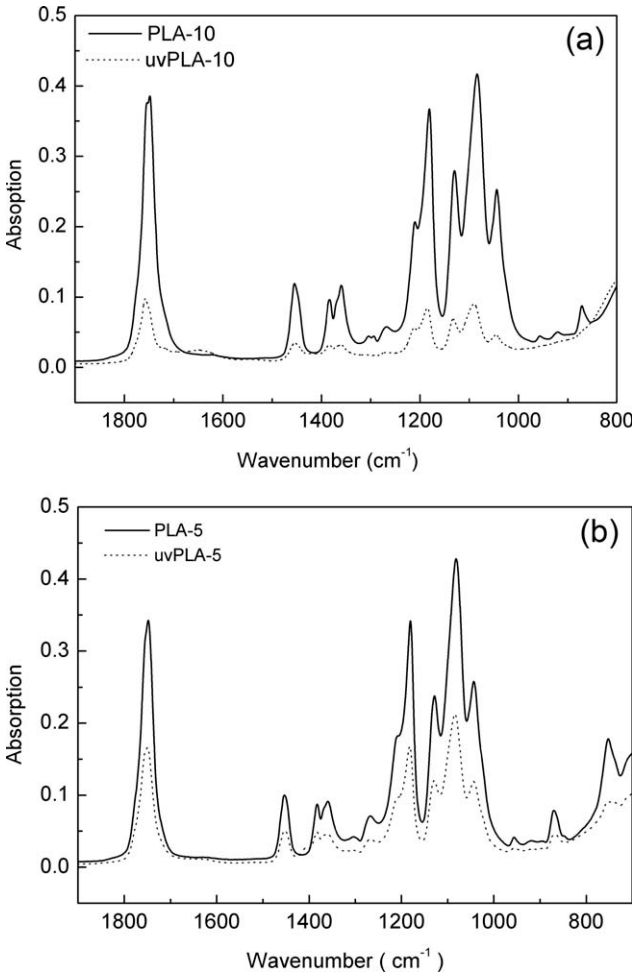

Figure 7 (a) FTIR-ATR spectra of UV irradiated (190 h) composite films containing 10 wt % TiO_2. (b) FTIR-ATR spectra of UV irradiated (190 h) composite films containing 5 wt % TiO_2.

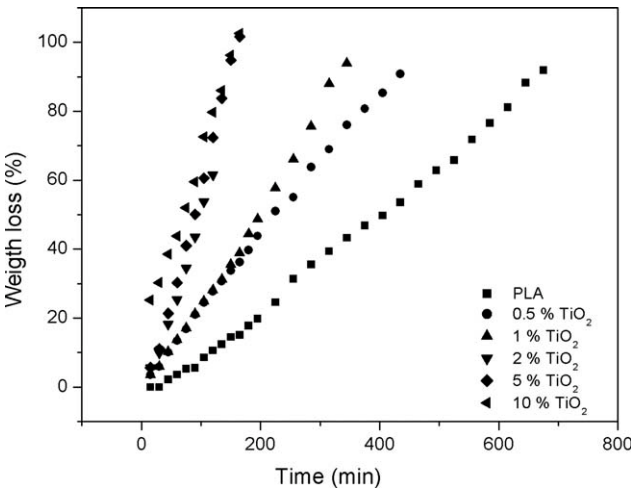

Figure 8 Weight loss (%)-time dependence (in 1 N NaOH) for PLA composites.

Hydrolytic degradation

Figure 8 shows the weight loss of PLA and its composite films as a function of exposed time in hydrolytic test. The degradation of PLA was completed in about 720 min, while the PLA composite films were hydrolyzed faster than neat PLA. Theoretically, films

TABLE IV
Results Obtained by Linear Fitting of Weigh Loss (%)–Time Graphs for Hydrolytic Degradation of PLA/TiO_2 Composite Films

Sample	Slope	*R*	SD
PLA	0.14	0.99	1.63
PLA-0.5	0.21	0.99	1.31
PLA-1	0.27	0.99	2.11
PLA-2	0.55	0.99	1.82
PLA-5	0.66	0.99	1.97
PLA-10	0.53	0.99	1.17

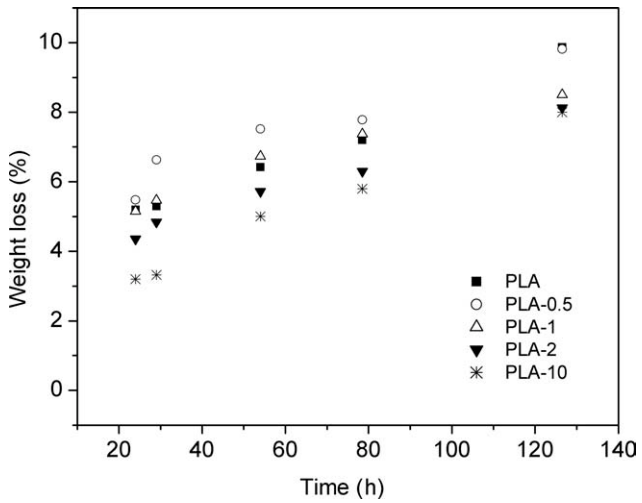

Figure 9 Weight loss-time dependence for PLA/TiO_2 composite films immersed in α-amylase solutions.

containing TiO_2 would be expected to show slower degradation. Interestingly, PLA/TiO_2 composites films exhibited much higher weight loss as a function of time than pure PLA resin. As shown in Figure 8, linear trend can be observed in the relation between weight loss and exposure time in the early stage of degradation. The hydrolytic degradation rates (Table IV) were defined as the slopes obtained by linear fitting of the weight loss (%) versus time plots given in Figure 8. PLA films containing higher content of TiO_2 were comparatively more hydrolytically degradable that pure PLA resin. Thus, it could be concluded that the hydrolytic rates of PLA nano composite films can be widely controlled by TiO_2 content.

Enzymatic degradation

Figure 9 shows normalized weight loss after exposure of PLA composite films in α-amylase solutions. It is interesting to note that the presented plots (weight loss % versus time) are linear. The highest extent of degradation after 126 h of exposure was detected in order as follows: PLA-0.5>PLA-1> PLA> PLA-2>PLA-10. Therefore it can be concluded that a dominant factor, determining the PLA enzymatic degradation, might be the diffusion controlled process, suppressed by increasing the filler content, acting as a blocker for larger molecules (such as α-amylase).

CONCLUSIONS

In this study, PLA/TiO_2 nanocomposites with different content of TiO_2 were prepared by solution casting method. SEM microscopy analysis shows that the TiO_2 nanoparticles are well dispersed in the PLA matrix with a limited tendency for forming aggregates smaller than 0.2 μm. The DSC results have shown that nanofillers have no significant influence on PLA's characteristic temperatures, (T_g, T_c, and T_m), but have significant effect on its crystallinity up to 5 wt % of TiO_2 loadings. The degradation experiments have shown an important influence of the TiO_2 loadings on the photodegradation acceleration, as well as on the hydrolytic degradation. The opposite effect was detected during the enzymatic degradation, suggesting that nanoparticles hinder diffusion of large molecules, such as α-amylase.

References

1. Ikada, Y.; Tsuju, H. Macromol Rapid Commun 2000, 21, 117.
2. Avella, M.; Buzarovska, A.; Errico, M.; Gentile, G.; Grozdanov, A. Materials 2009, 2, 911.
3. Weir, N. A.; Buchanan, F. J.; Orr, J. F.; Farrar, D. F.; Dickson, G. R. J Eng Med 2004, 218, 321.
4. Aon, K.; Hsu, S. L. Macromolecules 2006, 39, 3337.
5. Xu, Q.; Pang, M.; Peng, Q.; Jiang, Y.; Li, J.; Wang, H.; Zhu, M. J Appl Polym Sci 2005, 98, 831.
6. Zhou, Q.; Xanthos, M. Polym Degrad Stabil 2008, 93, 1450.
7. Gonzales, M. F.; Ruseckaite, R. A.; Cuadrato, T. R. J Appl Polym Sci 1999, 71, 1223.
8. Paul, M. A.; Delcourt, C.; Alexandre, M.; Degee, P.; Moteverde, F.; Dubois, P. Polym Degrad Stabil 2005, 87, 535.
9. Shogren, R. L.; Doane, W. M.; Garlotta, D.; Lawton, J. W.; Willett, J. L. J Polym Degrad Stabil 2003, 79, 405.
10. Ikada, E. J Photopolym Sci Technol 1998, 11, 23.
11. Ikada, E. J Photopolym Sci Technol 1998, 12, 251.
12. Tsuji, H.; Echizen, Y.; Nishimura, Y. Polym Degrad Stabil 2006, 91, 1128.
13. Copinet, A.; Bertrand, C.; Longieras, A.; Coma, V.; Couturier, Y. J Polym Environ 2003, 11, 169.
14. Yang, K.; Wang, X.; Wang, Y. J Ind Eng Chem 2007, 13, 485.
15. Reijnders, L. Polym Degrad Stabil 2009, 94, 873.
16. Pandey, J. K.; Reddy, K. R.; Kumar, A. P.; Singh, R. P. Polym Degrad Stabil 2005, 898, 234.
17. Chen, X. D.; Wang, Z.; Liao, Z. F.; Mai, Y. L.; Zhang, M. Q. Polym Test 2007, 26, 202.
18. Zhuang, W.; Liu, J.; Zhang, J. H.; Hu, B. X.; Shen, J. Polym Compos 2009, 30, 1074.
19. Song, M.; Pan, C.; Chen, C.; Li, J.; Wang, X.; Gu, Z. Appl Surf Sci 2008, 255, 610.
20. Nakayama, N.; Hayashi, T. Polym Degrad Stabil 2007, 92, 1255.
21. Qian, J.; Zhu, L.; Zhang, J.; Whitehouse, R. J Polym Sci B Polym Phys 2007, 45, 1564.
22. Fisher, E. W.; Sterzel, H. J.; Wegner, G. Colloid Polym Sci 1973, 251, 980.
23. Mandelkern, L. Crystallization of Polymers, Vol. 2; Cambridge University Press: UK, 2004.
24. Furukawa, T.; Sato, H.; Murakami, R.; Zhang, J.; Noda, I.; Ochiai, S.; Ozaki, Y. Polymer 2007, 48, 1749.
25. Blomergen, S.; Holden, D.; Hamer, G.; Bluhm, T.; Marchessault, R. Macromolecules 1986, 19, 2865.
26. Krevelen, D. W. Properties of Polymers; Elsevier Science: New York, 1990; Chapter 19.
27. Ha, C. S.; Cho, W. J Prog Polym Sci 2002, 27, 759.